

# Solution-Phase Extraction of Ultrathin Inner Shells from Double-Wall Carbon Nanotubes

Yasumitsu Miyata, Marie Suzuki, Miho Fujihara, Yuki Asada, Ryo Kitaura, and Hisanori Shinohara\*

Department of Chemistry, Nagoya University, Furo-cho, Chikusa-ku, Nagoya 464-8602, Japan

Carbon nanotubes (CNTs) are one-dimensional carbon materials and have recently attracted much attention because of their excellent mechanical and electrical properties.<sup>1</sup> It is well-known that CNTs can be classified into single-wall and multiwall CNTs (SWCNTs and MWCNTs). The structure of SWCNTs is regarded as having geometries of a rolled-up graphene sheet. The currently employed synthesis methods generally produce SWCNTs with a diameter of 0.7–3.0 nm.<sup>2–7</sup> MWCNTs are composed of SWCNT shells, and each shell is stably bound with each other by van der Waals interactions. Because of a wide variety of shell diameters in MWCNTs from 0.4 nm to several tens of nanometers,<sup>8</sup> the separation and extraction of each shell from a MWCNT could provide a novel way to prepare SWCNTs of very thin diameters. Importantly, these ultrathin tubes have been difficult to obtain from presently available growth methods of SWCNTs.

So far, some pioneering works have reported separation of inner tubes from an individual MWCNT using nanomanipulation techniques. In an early report, the extraction was demonstrated in a high-resolution transmission electron microscopy (HRTEM) with a nanomanipulator.<sup>9</sup> This technique was applied to prepare SWCNTs of an extremely large diameter (*ca.* 8 nm).<sup>10</sup> Recently, Hong *et al.* used an atomic-force microscopic approach to extract a subnanometer SWCNT from a MWCNT on a substrate.<sup>11</sup> These approaches are based on low intershell friction forces.<sup>12</sup> Although these manipulation approaches have allowed us to separate a single MWCNT, no efficient separation method has so far been reported for bulk CNT samples.

**ABSTRACT** We present an efficient method to extract inner shells of double-wall carbon nanotubes (DWCNTs) in liquid phase. The extraction of inner from outer shells is achieved by cutting the DWCNTs with vigorous sonication in water containing surfactants. The extracted shells are perfectly isolated single-wall carbon nanotubes (SWCNTs) and can be separated using density gradient ultracentrifugation. Statistical analysis using high-resolution transmission electron microscopy reveals that the enrichment of SWCNTs with narrow diameter (0.62–1.0 nm) up to 100% is achieved from highly pure DWCNTs. Furthermore, the (5,4) SWCNTs, which have the diameter of 0.62 nm, are concentrated. Our findings provide a novel way to obtain very narrow, highly isolated SWCNTs with ultraclean surface that have not been obtained in conventional synthesis methods.

**KEYWORDS:** single-wall carbon nanotubes · double-wall carbon nanotubes · separation · density gradient ultracentrifugation · transmission electron microscopy

In this study, we demonstrate an efficient method to separate inner and outer shells in double-wall CNTs (DWCNTs) using ultrasonication and ultracentrifugation processes. The extraction of inner shells is achieved by cutting the DWCNTs with vigorous sonication in water containing surfactants. The extracted shells so-produced are perfectly isolated SWCNTs encapsulated by surfactants and can readily be separated by using density gradient ultracentrifugation (DGU), which has been applied for the sorting of CNTs by diameter, chirality, and shell number (types) of CNTs.<sup>13,14</sup> Our findings provide an effective way to produce unique SWCNTs with very small/large diameter, surface impurity free, and perfectly isolated state.

## RESULTS AND DISCUSSION

In the present study, the shell extraction was carried out with vigorous sonication treatment for high-purity DWCNT samples (hereafter refer to as DW-sample). To confirm the extraction of inner shells from DWCNTs, we measured abundances of SWCNTs and DWCNTs for the DW-sample through HRTEM observations. Figure 1b–g

\*Address correspondence to noris@nagoya-u.jp.

Received for review July 8, 2010 and accepted September 01, 2010.

Published online September 9, 2010. 10.1021/nn1015665

© 2010 American Chemical Society

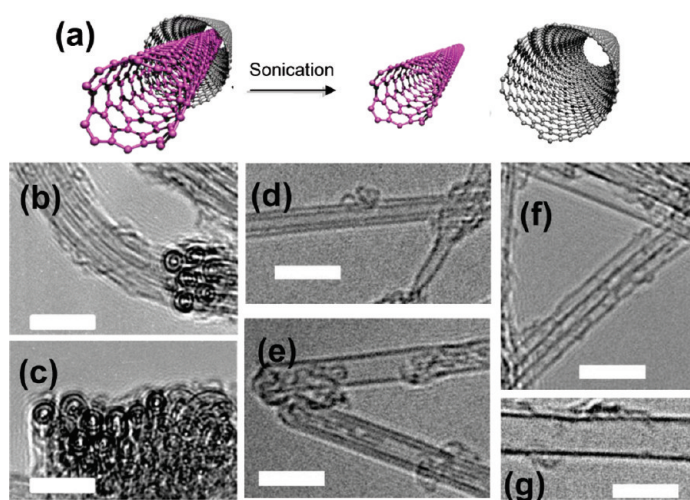


**Figure 1.** (a) Schematic illustration of the separation of inner and outer shells in DWCNTs. (b) Typical HRTEM images of DW-samples (b,c) before and (d–g) after the sonication treatment. The scale bar is 5 nm.

shows typical HRTEM images of CNTs observed for the DW-sample before and after the sonication. The number of SWCNTs and DWCNTs observed for each sample was summarized in Table 1. In the pristine DW-sample, the ratio of SWCNTs and DWCNTs was less than ca. 5%. The ratio of SWCNTs, however, drastically increased to 50% after the sonication.

The diameter distribution of these two samples was investigated to obtain information as to whether the observed SWCNTs correspond to the extracted shells from DWCNTs. Figure 2 presents the histograms of diameter distribution of SWCNTs and DWCNTs in the DW-sample before and after the sonication. For the pristine DW-sample, the average diameters of the outer and inner tubes of the DWCNTs were found to be 1.6 and 0.8 nm, respectively (Figure 2a). Determining the diameter distribution of SWCNTs was not possible because of their small amount in the pristine DW-sample. The histogram of DWCNTs after the sonication (Figure 2d) is almost the same as that before the sonication. Importantly, the histogram of SWCNTs after the sonication also shows bimodal peaks at 0.7 and 1.6 nm as shown in Figure 2f. The bimodal peaks are very similar to the sum of inner and outer shells of DWCNTs (Figure 2b,e). These results strongly support that the increase of SWCNTs after the sonication is indeed caused by the extraction of inner shells from DWCNTs.

The extraction may well be resulted from the partial cutting of outer shells of DWCNTs at the time of sonication, which is followed by the mutual sliding of inner and outer shells. This sliding can be accelerated by

the shock waves formed under the sonication. It is well-known that the sonication treatment can produce shortening and cutting of CNTs.<sup>15</sup> An image of this partial cutting has actually been obtained for the MWCNTs by the HRTEM observations.

Figure 3 shows HRTEM images of MWCNT samples before and after the sonication. For the pristine sample, all the observed MWCNTs possess a closed cap at the end of tubes as shown in Figure 3a. After the sonication, partially protruding inner shells were frequently found for a MWCNT (Figure 3b). These images strongly suggest that the sonication can cut and peel off a part of outer shells of MWCNTs and separate them from the inner shells. The partial separation of the shells of the MWCNT has been seen only for the MWCNTs which are known to possess locally imperfect concentric structures. In contrast, it has never been observed for the DWCNTs used which have almost perfect concentric structure. This perfect concentric structure likely causes a smooth sliding of the mutual shells of DWCNTs due to very low intershell friction forces.<sup>12</sup>

We have also found that the extracted inner shells can be effectively sorted by using DGU. Figure 4a shows photographs of the DW-sample dispersion in the centrifuge tube before and after the DGU. The sample was fractionated as shown in Figure 4a and evaluated by using HRTEM, optical absorption, and Raman scattering. The HRTEM images show that fraction 1 contains only SWCNTs with narrow diameter (Figure 4b,c). Their diameter distribution is found to be 0.6–1.0 nm (Figure 4d), which well agrees with the distribution of inner shells of DWCNTs as shown in Figure 2a,b. On the other hand, the higher density fractions contain both SWCNTs with a large diameter and DWCNTs.

Figure 4 panels e and f show the Raman spectra of fraction 1 and the unseparated dispersion before the DGU. For the unseparated sample, radial breathing mode (RBM) Raman peaks are observed from 140 to 370  $\text{cm}^{-1}$  in the two spectra, indicating that the sample

**TABLE 1. The Numbers of Observed SWCNTs and DWCNTs for the Pristine and the Sonicated DW-Samples**

sample	pristine	sonicated
$N_{\text{total}}$	113	384
$N_{\text{DWCNT}}$	109 (96%)	190 (49%)
$N_{\text{SWCNT}}$	4 (4%)	194 (51%)

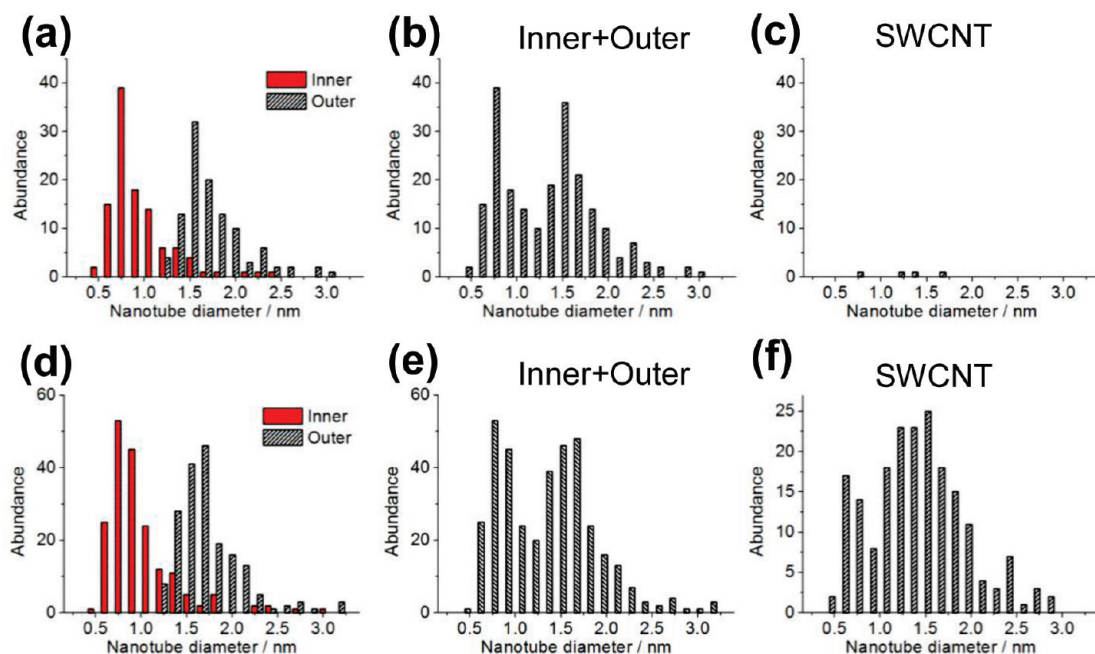


Figure 2. The histogram of diameter distributions of inner and outer shells in DWCNTs and SWCNTs for (a–c) the pristine and (d–f) the sonicated DW-samples.

mainly contains CNTs with a diameter distribution of 0.6–1.7 nm.<sup>16,17</sup> In contrast, fraction 1 shows the RBM peaks only between 280 and 370  $\text{cm}^{-1}$ , which corresponds to the diameter from 0.8 to 0.6 nm. In the high-energy region, the tangential mode (G-mode) and defect-induced Raman mode (D-mode) were seen around 1590 and 1300  $\text{cm}^{-1}$ , respectively, for both the samples. Interestingly, fraction 1 shows an almost vanishing D-mode peak, suggesting high quality (crystallinity) of the inner shells extracted by the present method.

A high degree of the current separation can also be confirmed from the optical absorption spectra. Figure 4g is the optical absorption spectra of the unseparated dispersion and fraction 1. In the region of 1300–900 nm, the unseparated part of dispersion shows a broad absorption peak with fine structure. This broad peak is actually a superposition of excitonic optical absorptions of inner shell  $S_{11}$  band and outer shell  $S_{22}$  band, whereas fraction 1 displays several sharp absorption peaks. These sharp peaks originate from only the  $S_{11}$  bands of the separated inner shells. From the experimental *k*-taura plot proposed by Weisman *et al.*,<sup>18</sup> the chiral index of each sharp peak can be assigned as shown in Figure 4g. From this assignment, the diameter distribution is evaluated to be 0.62–1.0 nm. Both the Raman and absorption results are completely consistent with the result of HRTEM observations.

Very interestingly, the absorption spectrum reveals that the SWCNTs having a chirality of (5,4), which corresponds to a very narrow diameter of 0.62 nm, are one of the major components in the extracted inner shells. This is quite different from the well-known SWCNT samples of narrow diameters produced by the HiPco<sup>19,20</sup> and CoMoCAT methods.<sup>2</sup> In these samples, the absorption peak of (5,4) SWCNTs has never been observed

even after the separation process.<sup>21</sup> Although one previous study has reported quantitative photoluminescence (PL) analysis of such SWCNTs, the relative PL intensity detected is only 0.3% of the total PL intensities of semiconducting SWCNTs included in the sample.<sup>2</sup> This suggests the (5,4) SWCNTs are extremely unstable under the conventional synthesis condition, which normally requires high temperatures above 600 °C. One of the main causes of such instability is due to their large curvature along the C–C bond, that is, the large  $\pi$ -orbital axis vector (POAV) as proposed by Haddon.<sup>22</sup> Such unstable nanotubes should, however, become stable in the presence of surrounding outer shells and stably grow as inner shells of DWCNTs. We think that this is the main reason why the present fraction contains very narrow SWCNTs.

In the present study, we have achieved the further enrichment of the (5,4) SWCNTs using fine-tuned density gradient separation as reported by Ghosh *et al.*<sup>21</sup> The improved DGU allows us to obtain various colorful layers as shown in Figure 5a. Figure 5b shows the optical absorption spectrum of (5,4)-enriched fraction. Two distinct peaks corresponding to (5,4) and (6,4) SWCNTs

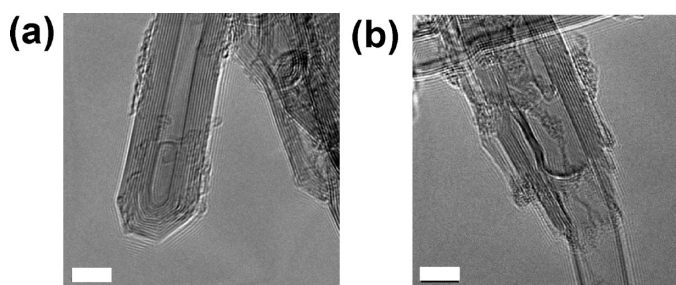


Figure 3. HRTEM images of MWCNTs (a) before and (b) after the sonication treatment. The scale bar is 5 nm.

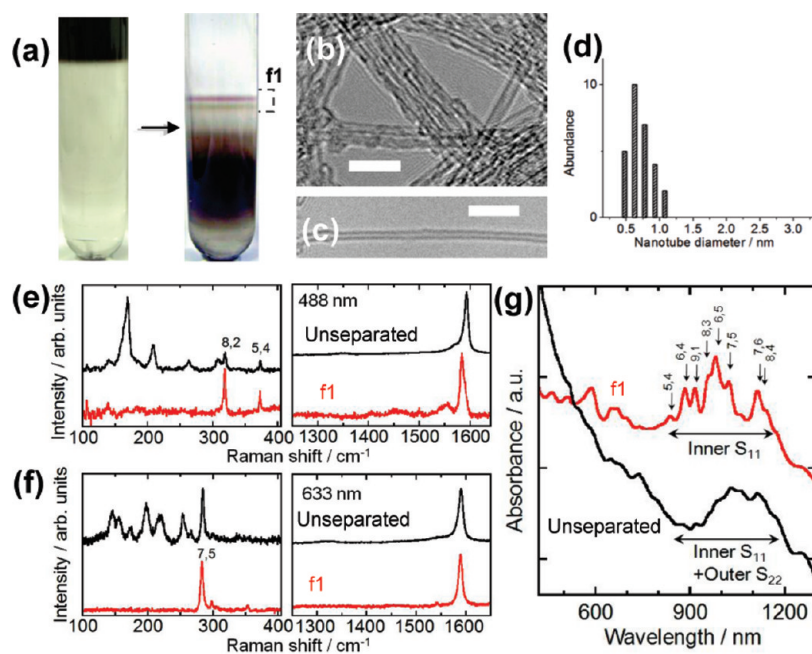


Figure 4. (a) Photographs of the centrifugal tubes (left) before and (right) after the density gradient ultracentrifugation process. Fraction 1 (f1) corresponds to the part indicated by dashed line. (b,c) Typical HRTEM images and (d) the histogram of diameter distributions of CNTs in fraction 1. The scale bar is 5 nm. (e,f) Raman and (g) optical absorption spectra of fraction 1 and unseparated dispersion. Raman spectra were measured at the laser excitation wavelength of (e) 488 nm and (f) 633 nm.

can be seen at 835 and 880 nm, respectively. This further shows that the present solution-phase extraction of inner shells is a very effective way to obtain ultrathin SWCNTs that have never been obtained in the conventional synthesis methods of SWCNTs.

Finally, it is noted that our results raise a question whether or not inner shells in DWCNTs can exhibit PL. Although several groups including our own<sup>23</sup> have reported the observation of strong PL from inner shells of DWCNTs, all of the studies prepared the PL samples with strong sonication treatment for the isolation of DWCNTs.<sup>23–26</sup> This process may possibly have led to extraction of inner shells from DWCNTs, which is followed by emitting PL from such SWCNTs. Meanwhile,

some other groups have reported that the highly enriched DWCNTs by DGU show much weaker PL than SWCNTs.<sup>14,27</sup> Tsyboulski *et al.* reported that the PL intensity of inner shells is 10 000 times as weak as that of SWCNTs and that inner shells may be exposed or released from DWCNTs during extensive chemical and physical treatment.<sup>27</sup> The present study experimentally confirms efficient extraction of the inner shell from DWCNTs and can provide a rationale for the mutually contradicting previous reports on the inner shell emission of DWCNTs.

## CONCLUSION

We have presented an efficient and simple method to separate inner shells from outer shells of DWCNTs. The inner shells are extracted in solution phase by using vigorous sonication and separated using DGU. The present method provides a novel way to produce unique SWCNTs with very small/large diameters, high quality, and perfectly isolated state. The present technique may also provide opportunities to extract ultranarrow SWCNTs embedded in other supporting materials such as zeolite.<sup>28</sup> The isolation of such narrow SWCNTs allows us to investigate their intrinsic transport properties related to superconductivity as well as exotic electrical and optical natures with strong quantum confinement.

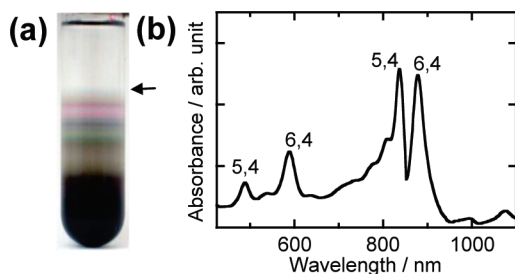


Figure 5. (a) Photograph of the centrifugal tube after the improved density gradient ultracentrifugation process. (b) Optical absorption spectrum of the part indicated by an arrow in panel a.

## EXPERIMENTAL DETAILS

The DWCNT-sample was supplied from Toray Industries Inc. This material was synthesized by using catalyst-supported chemical vapor deposition (CCVD) method and purified by ther-

mal oxidation in air as reported by Kishi *et al.*<sup>29</sup> The MWCNT-sample was produced by CCVD previously reported.<sup>30,31</sup> The MWCNTs were high-temperature annealed at 2000 °C to obtain better crystallinity of the nanotubes. For the DW-sample, the pu-

rity of DWCNTs (against residual SWCNTs and MWCNTs) is more than 90%, and the average diameters of the outer and inner tubes of the DWNTs are 1.6 and 0.8 nm, respectively, based on HRTEM observations. For the MWCNT sample, the purity of MWCNTs is 100% (without SWCNTs and DWCNTs) based on HRTEM observations.

For the shell extraction, the DW sample (3 mg) was dispersed in H<sub>2</sub>O (20 mL) with 1% weight per volume (w/v) sodium cholate hydrate (SC, 99% Sigma-Aldrich) using an ultrasonic homogenizer (Sonifire 450D, Branson, power density of 20 W/cm<sup>2</sup>) for 18 h. The MW-sample (3.0 mg) was sonicated for 25 h in H<sub>2</sub>O (20 mL) with 2% w/v SC. During the sonication, the solution was immersed in a bath of cold water to prevent heating. The solution was centrifuged at 197000g for 15 min using a swing bucket S52ST rotor (Hitachi Koki). The upper 80% of the supernatant was then corrected and used for the DGU reported by Hersam and colleagues.<sup>13,14</sup> In the DGU process, the surfactant concentration was kept to 2% w/v SC and 30% w/v iodixanol (purchased as OptiPrep from Daiichi Pure Chemicals Co.). This sample dispersion (1 mL) was placed between the step density gradients which were formed from aqueous solutions of iodixanol in a centrifuge tube, varying from 20% w/v (2 mL) at the top to 40% w/v (2 mL) at the bottom with the same surfactant concentration to that of the sample. After centrifugation at 197000g for 15 h, the solution was fractionated using a pipet. To measure optical absorption and Raman scattering, the iodixanol was removed from the sample solution through filtration using centrifugal filter devices (Amicon Ultra, 100000 NMWL, Millipore). The samples were dispersed again in D<sub>2</sub>O with sonication. In the improved DGU process, the sample dispersion (1.3 mL, 25% w/v iodixanol, 1% w/v SC) was put in the step gradients which were prepared from layers with the following iodixanol concentrations and volumes: 30% (1 mL), 22.5% (0.66 mL), 20.0% (0.66 mL), 17.5% (0.7 mL), and 15.0% (0.8 mL). The surfactant concentration in this gradient was fixed at 1% w/v SC.

Optical absorption spectra were measured using a UV–vis spectrophotometer (V-570, JASCO). Raman spectra were measured in a backscattering geometry using a single monochromator (HR-800, Horiba Jobin Yvon) equipped with a charge-coupled device detector and a notch filter. The samples were excited by an argon ion laser at 488 nm (2.54 eV) and a helium–neon laser at 633 nm (1.96 eV).

HRTEM observations were carried out on a JEM-2100F (JEOL) high-resolution field-emission gun TEM operated at 80 keV at room temperature and under a pressure of 10<sup>-6</sup> Pa. The sample solution was mixed with methanol to remove the surfactant from CNTs. The reference sample was dispersed in methanol by the weak sonication for 2 min with an ultrasonic bath sonicator. The solution was then dropped onto a copper grid coated with thin carbon film. The sample was heated at 50 °C under vacuum for 15 min to remove methanol and water just before the HRTEM observations. HRTEM images were recorded with a charge-coupled device with an exposure time of typically 1 s.

**Acknowledgment.** The authors thank M. Yoshikawa and K. Sato of Chemical Research Laboratories, Toray Industries, Inc. for preparation of highly pure DWCNTs. This work has been supported by the Grant-in-Aids for Specific Area Research (no. 19084008) on Carbon Nanotube Nano-Electronics and for Scientific Research A (no. 19205003) Education, Culture, Sports, Science and Technology (MEXT) of Japan and partly by the Akasaki foundation in Nagoya University. Y.M. acknowledges the financial support by a Grant-in-Aid for Young Scientists (Start-up) from the Japan Society for the Promotion of Science.

## REFERENCES AND NOTES

- Reich, S.; Thomsen, C.; Maultzsch, J. *Carbon Nanotubes: Basic Concepts and Physical Properties*; Wiley-VCH: Berlin, 2004.
- Bachilo, S. M.; Balzano, L.; Herrera, J. E.; Pompeo, F.; Resasco, D. E.; Weisman, R. B. Narrow (*n,m*)-Distribution of Single-Walled Carbon Nanotubes Grown Using a Solid Supported Catalyst. *J. Am. Chem. Soc.* **2003**, *125*, 11186–11187.
- Hata, K.; Futaba, D. N.; Mizuno, K.; Namai, T.; Yumura, M.; Iijima, S. Water-Assisted Highly Efficient Synthesis of Impurity-Free Single-Walled Carbon Nanotubes. *Science* **2004**, *306*, 1362–1364.
- Nikolaev, P.; Bronikowski, M. J.; Bradley, R. K.; Rohmund, F.; Colbert, D. T.; Smith, K. A.; Smalley, R. E. Gas-Phase Catalytic Growth of Single-Walled Carbon Nanotubes from Carbon Monoxide. *Chem. Phys. Lett.* **1999**, *313*, 91–97.
- Thess, A.; Lee, R.; Nikolaev, P.; Dai, H. J.; Petit, P.; Robert, J.; Xu, C. H.; Lee, Y. H.; Kim, S. G.; Rinzler, A. G.; *et al.* Crystalline Ropes of Metallic Carbon Nanotubes. *Science* **1996**, *273*, 483–487.
- Saito, T.; Ohshima, S.; Okazaki, T.; Ohmori, S.; Yumura, M.; Iijima, S. Selective Diameter Control of Single-Walled Carbon Nanotubes in the Gas-Phase Synthesis. *J. Nanosci. Nanotechnol.* **2008**, *8*, 6153–6157.
- Hong, B. H.; Lee, J. Y.; Beetz, T.; Zhu, Y.; Kim, P.; Kim, K. S. Quasi-Continuous Growth of Ultralong Carbon Nanotube Arrays. *J. Am. Chem. Soc.* **2005**, *127*, 15336–15337.
- Guan, L. H.; Suenaga, K.; Iijima, S. Smallest Carbon Nanotube Assigned with Atomic Resolution Accuracy. *Nano Lett.* **2008**, *8*, 459–462.
- Cummings, J.; Zettl, A. Low-Friction Nanoscale Linear Bearing Realized from Multiwall Carbon Nanotubes. *Science* **2000**, *289*, 602.
- Chang, Y. C.; Liaw, Y. H.; Huang, Y. S.; Hsu, T.; Chang, C. S.; Tsong, T. T. *In Situ* Tailoring and Manipulation of Carbon Nanotubes. *Small* **2008**, *4*, 2195–2198.
- Hong, B. H.; Small, J. P.; Purewal, M. S.; Mullokandov, A.; Sfeir, M. Y.; Wang, F.; Lee, J. Y.; Heinz, T. F.; Brus, L. E.; Kim, P.; *et al.* Extracting Subnanometer Single Shells from Ultralong Multiwalled Carbon Nanotubes. *Proc. Natl. Acad. Sci. U.S.A.* **2005**, *102*, 14155–14158.
- Kolmogorov, A. N.; Crespi, V. H. Smoothest Bearings: Interlayer Sliding in Multiwalled Carbon Nanotubes. *Phys. Rev. Lett.* **2000**, *85*, 4727–4730.
- Arnold, M. S.; Green, A. A.; Hulvat, J. F.; Stupp, S. I.; Hersam, M. C. Sorting Carbon Nanotubes by Electronic Structure Using Density Differentiation. *Nat. Nanotechnol.* **2006**, *1*, 60–65.
- Green, A. A.; Hersam, M. C. Processing and Properties of Highly Enriched Double-Wall Carbon Nanotubes. *Nat. Nanotechnol.* **2009**, *4*, 64–70.
- Shelimov, K. B.; Esenaliev, R. O.; Rinzler, A. G.; Huffman, C. B.; Smalley, R. E. Purification of Single-Wall Carbon Nanotubes by Ultrasonically Assisted Filtration. *Chem. Phys. Lett.* **1998**, *282*, 429–434.
- Kataura, H.; Kumazawa, Y.; Maniwa, Y.; Umez, I.; Suzuki, S.; Ohtsuka, Y.; Achiba, Y. Optical Properties of Single-Wall Carbon Nanotubes. *Synth. Met.* **1999**, *103*, 2555–2558.
- Fantini, C.; Jorio, A.; Souza, M.; Strano, M. S.; Dresselhaus, M. S.; Pimenta, M. A. Optical Transition Energies for Carbon Nanotubes from Resonant Raman Spectroscopy: Environment and Temperature Effects. *Phys. Rev. Lett.* **2004**, *93*, 147406–1–4.
- Weisman, R. B.; Bachilo, S. M. Dependence of Optical Transition Energies on Structure for Single-Walled Carbon Nanotubes in Aqueous Suspension: An Empirical Kataura Plot. *Nano Lett.* **2003**, *3*, 1235–1238.
- O’Connell, M. J.; Bachilo, S. M.; Huffman, C. B.; Moore, V. C.; Strano, M. S.; Haroz, E. H.; Rialon, K. L.; Boul, P. J.; Noon, W. H.; Kittrell, C.; *et al.* Band Gap Fluorescence from Individual Single-Walled Carbon Nanotubes. *Science* **2002**, *297*, 593–596.
- Bachilo, S. M.; Strano, M. S.; Kittrell, C.; Hauge, R. H.; Smalley, R. E.; Weisman, R. B. Structure-Assigned Optical Spectra of Single-Walled Carbon Nanotubes. *Science* **2002**, *298*, 2361–2366.
- Ghosh, S.; Bachilo, S. M.; Weisman, R. B. Advanced Sorting of Single-Walled Carbon Nanotubes by Nonlinear Density-Gradient Ultracentrifugation. *Nat. Nanotechnol.* **2010**, *5*, 443–450.
- Haddon, R. C. Hybridization and the Orientation and Alignment of  $\pi$ -Orbitals in Nonplanar Conjugated Organic Molecules:  $\pi$ -Orbital Axis Vector Analysis (POAV2). *J. Am. Chem. Soc.* **1986**, *108*, 2837–2842.

23. Kishi, N.; Kikuchi, S.; Ramesh, P.; Sugai, T.; Watanabe, Y.; Shinohara, H. Enhanced Photoluminescence from Very Thin Double-Wall Carbon Nanotubes Synthesized by the Zeolite-CCVD Method. *J. Phys. Chem. B* **2006**, *110*, 24816–24821.
24. Hertel, T.; Hagen, A.; Talalaev, V.; Arnold, K.; Hennrich, F.; Kappes, M.; Rosenthal, S.; McBride, J.; Ulbricht, H.; Flahaut, E. Spectroscopy of Single- and Double-Wall Carbon Nanotubes in Different Environments. *Nano Lett.* **2005**, *5*, 511–514.
25. Shimamoto, D.; Muramatsu, H.; Hayashi, T.; Kim, Y. A.; Endo, M.; Park, J. S.; Saito, R.; Terrones, M.; Dresselhaus, M. S. Strong and Stable Photoluminescence from the Semiconducting Inner Tubes within Double Walled Carbon Nanotubes. *Appl. Phys. Lett.* **2009**, *94*, 083106–1-3.
26. Kim, J. H.; Kataoka, M.; Shimamoto, D.; Muramatsu, H.; Jung, Y. C.; Hayashi, T.; Kim, Y. A.; Endo, M.; Park, J. S.; Saito, R.; *et al.* Raman and Fluorescence Spectroscopic Studies of a DNA-Dispersed Double-Walled Carbon Nanotube Solution. *ACS Nano* **2010**, *4*, 1060–1066.
27. Tsybouski, D. A.; Hou, Y.; Fakhri, N.; Ghosh, S.; Zhang, R.; Bachilo, S. M.; Pasquali, M.; Chen, L. W.; Liu, J.; Weisman, R. B. Do Inner Shells of Double-Walled Carbon Nanotubes Fluoresce. *Nano Lett.* **2009**, *9*, 3282–3289.
28. Lortz, R.; Zhang, Q.; Shi, W.; Ye, J. T.; Qiu, C.; Wang, Z.; He, H.; Sheng, P.; Qian, T.; Tang, Z.; *et al.* Superconducting Characteristics of 4-A Carbon Nanotube–Zeolite Composite. *Proc. Natl. Acad. Sci. U.S.A.* **2009**, *106*, 7299–7303.
29. Kishi, N.; Hiraoka, T.; Ramesh, P.; Kimura, J.; Sato, K.; Ozeki, Y.; Yoshikawa, M.; Sugai, T.; Shinohara, H. Enrichment of Small-Diameter Double-Wall Carbon Nanotubes Synthesized by Catalyst-Supported Chemical Vapor Deposition Using Zeolite Supports. *Jpn. J. Appl. Phys.* **2007**, *46*, 1797–1802.
30. Mukhopadhyay, K.; Koshio, A.; Tanaka, N.; Shinohara, H. A Simple and Novel Way to Synthesize Aligned Nanotube Bundles at Low Temperature. *Jpn. J. Appl. Phys.* **1998**, *37*, L1257–L1259.
31. Mukhopadhyay, K.; Koshio, A.; Sugai, T.; Tanaka, N.; Shinohara, H.; Konya, Z.; Nagy, J. B. Bulk Production of Quasi-Aligned Carbon Nanotube Bundles by the Catalytic Chemical Vapour Deposition (CCVD) Method. *Chem. Phys. Lett.* **1999**, *303*, 117–124.